Design of a load following management for a PWR reactor using an optimization method

Mathieu Muniglia, Le Pallec Jean-Charles, Jean-Michel Do, Sebastien Verel

M&C 2017 - International Conference on Mathematics & Computational Methods Applied to Nuclear Science & Engineering, Jeju, Korea, April 16-20, 2017, on USB (2017)

Design of a load-following management for a PWR reactor using an optimization method

Mathieu Muniglia*, Jean-Charles Le Pallec*, Jean-Michel Do*, Sébastien Verel†

*Commissariat à l'Energie Atomique, F-91191 Gif-Sur-Yvette, France
†Univ. du Littoral Côte d'Opale, F-62100 Calais, France
mathieu.muniglia@cea.fr

Abstract - *In this paper, an optimization of the control rods parameters of a nuclear power plant is presented. Using a multi-physics simulator, the criteria of interest are computed in few minutes of computation and the optimization problem is solved thanks to a parallel asynchronous master-worker* $(1 + \lambda)$*-Evolutionary Algorithm. Two criteria are minimized independently: the first one based on the control diagram is a measure of the energy heterogeneity of the core, and a second one corresponding to the volume of effluents resulting from the use of the soluble boron. The main goal of this paper is then to analyze the solutions found by the optimization. Moreover, it is known that the burnup of the core has a strong influence on the use of the soluble boron, so different starting points have been considered, showing that the evolution of the performances of the good solutions as regards the two criteria are not the same. Finally, this paper shows that two gathered mono-objective optimizations are not satisfactory enough if one considers the burnup evolution, and that a bi-objective optimization must be considered to solve this problem.*

I. INTRODUCTION

In the actual context of energetic transition, the increase of the intermittent renewable energies contribution (as wind farms or solar energy) is a major issue. On the one hand, the French government aims at increasing their part up to 30% [1] by 2030, against 6% today. On the other hand, their intermittent production may lead to an important imbalance between production and consumption. Consequently, the other ways of production must adapt to those variations, especially nuclear energy which is the most important in France. The power variations occur at different time scales (hour, day, or even week) and in order to counterbalance their effects on the electric grid, the nuclear power plants (NPP) are already able to adjust their production. NPPs which take part in the response of the power variations operate in the so-called load-following mode. In this operating mode, the power plant is controlled using control rods (neutron absorber) or soluble boron. However, the control rods may introduce unacceptable spatial perturbations in the core, especially if the power variations are large and/or fast, and the use of the soluble boron produces waste effluents that need to be processed. The purpose of this work is to optimize the manageability of the power plants to cope with a large introduction of intermittent renewable energies, and its final goal is to tune the control parameters in order to be able to make the load-following at a shorter time scale and larger power amplitude scale, or increase the safety margins to do so.

Such an optimization is a real challenge, considering the size of the search domain, the computation cost and the unknown properties of the objective function to minimize. Due to the design of the nuclear power plants, and in a goal to propose only simple modifications of the current management, 11 integer variables are used to describe the control rods such as speed, overlaps between rods, etc. (details are given in Sect. II.). The soluble boron use will be a consequence of those parameters selection. Therefore, the optimization is a large size combinatorial problem where no full enumeration is possible. Moreover, a multi-physics simulator is used to compute according to the variables of the main parameters of the control rods several criteria such as the evolution of the axial power offset, the rejected volume of effluent, etc.

The use of Evolutionary Algorithms (EA) in order to optimize some variables of a nuclear power plant as regards performance or safety is not new. Offline optimizations can already be found, and studies such as [2] or [3] deal with the In-Core Fuel Management Optimization (ICFMO) and loading pattern optimization which is a well-known problem of Nuclear Engineering and aims for instance at maximizing the use of the fuel (increase the cycle length for example) while keeping the core safe (minimize the power peak). Pereira and Lapa consider in [4] an optimization problem that consists in adjusting several reactor cell variables, such as dimensions, enrichment and materials, in order to minimize the average peak-factor in a reactor core, considering some safety restrictions. This is extended in [5] to stochastic optimization algorithms conceptually similar to Simulated Annealing. Sacco *et al.* even perform in [6] an optimization of the surveillance tests policy on a part of the secondary system of a Nuclear Power Plant, using a metaheuristic algorithm, which goal is to maximize the system average availability for a given period of time.

To the best authors' knowledge, the only optimizations of the plant operation are made online, like in [7], where Na *et al.* develop a fuzzy model predictive control (MPC) method to design an automatic controller for thermal power control in pressurized water reactors. The objectives are to minimize both the difference between the predicted reactor power and the desired one, and the variation of the control rod positions. A genetic algorithm is then used to optimize the fuzzy MPC. Kim *et al.* propose in [8] another MPC by applying a genetic algorithm, to optimize this time the discrete control rod speeds. The offline Nuclear Reactor Operation Optimization (NROO) proposed in this paper and using an Evolutionary Algorithm (EA) is then an original combinatorial black-box problem. Moreover, the black-box objective function, which is also called fitness function in the context of

evolutionary computation, is computationally expensive (one evaluation typically takes on average about 40 minutes) so that only few candidate solutions and their corresponding fitness value, which is the value of the criterion, can be computed. Otherwise, no property on the search space is *a priori* known.

With the increasing number of computing resources (cores, gpgpu, etc.), EAs which are population-based stochastic optimization algorithm, and more specifically parallel EAs become more and more popular to solve complex optimization problems. Usually, parallel EA [9] can be classified into two main models: the coarse-grained model (or island model) in which several EA share candidate solutions within the migration process, and the fine-grained model (or cellular model) where the search population is spread into a grid and evolutionary operators are locally executed. Moreover, the execution of parallel EA follows two main architectures. In the P2P architecture, the computation is fully distributed on all computation units, and in the Master-Worker (M/W) architecture, the fitness evaluation is on workers. The M/W architecture has been extensively used and studied [10]. It is simple to implement, and does not require sophisticated parallel techniques and communications. Two communication modes are usually considered. In the synchronous mode, the parallel algorithm is organized by round. The master sends candidate solutions on each worker for evaluation, and waits until receiving a response from all workers before the next round. In the asynchronous mode, the master does not need to wait, and communicates individually with each worker on-the-fly. The asynchronous mode could improve the parallel efficiency when the evaluation time of the fitness function vary substantially [11]. In this paper, an asynchronous M/W parallel EA is used to solve the NROO problem.

The main goals of the paper are then : (i) perform for the first time an optimization of the control rods using an evolutionary algorithm (ii) analyze the efficient solutions as regards an axial offset criterion as well as the effluents volume and (iii) study the suitability of a bi-objective optimization.

The rest of this paper is organized as follows. The next section introduces the NROO problem, that is to say the tunable parameters and the criteria. The proposed algorithm is described in Sect. III., and in Sect. IV., the experimental analysis of the found solutions is conducted. At last, the paper concludes on the main results, and future works.

II. PROBLEM DEFINITION

The optimization process is based on the current load-following transient [12] and this analysis focuses on a single Pressurized Water Reactor (PWR) type (1300 MW) of the French nuclear fleet. The typical load-following transient considered here is presented on Fig.1, and corresponds to the most penalizing scenario in the specifications of a nuclear power plant.

In a general way, when an electrical power variation occurs (demand of the grid) a chain of feedback is setting up in the whole reactor, leading to a new steady state. It is usual to take advantage of this self-regulation in the case of small variations, but the regulated variables such as the temperature or the pressure in the primary or secondary circuits may reach

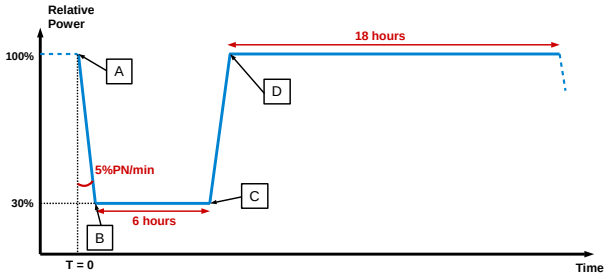

Fig. 1. Load-following scenario considered for this optimization exercise. It is made of a power decrease at $5\%PN/min$ to reach the lower plateau at $30\%PN$ (point B), then the power is kept constant during 6 hours (until point C) before coming back to nominal power (point D).

unacceptable values in case of such a load-following, possibly leading to damages of the whole system. The control rods are then used in order to cope with this variation, and maintain the primary coolant temperature close to the target. However, those control rods have to be handled carefully as they could cause axial or radial heterogeneity in the core, inducing high power peaks or Xenon oscillations.

1. Description of the System

The reactor core is a grid of square assemblies in a cylindrical vessel. Each assembly is 21 centimeters side length and about four meters high. There are 193 assemblies, split into two kinds : 120 assemblies made of Uranium oxide (UOX) and 73 ones made of Uranium plus Gadolinium oxides (UGd). Fig.2 shows the core of the reactor : the UOX assemblies are in orange, the UGd ones in purple, and the green stands for the steel vessel.

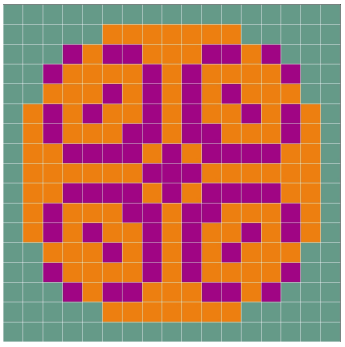

Fig. 2. Position of the types of assemblies in a typical PWR1300.

Each control rod is made of pins of a neutron absorber that are inserted together from the top of the core in some assemblies. The positions of the assemblies where they are inserted and the materials of which they are made correspond to the French "G" mode [12]. There are two kinds of rods in this "G" mode : the *black* rods made of very absorbing pins (B_4C and Ag+In+Cd) and the *gray* rods (giving their name

to the mode), made of less absorbing pins (stainless steel and *Ag+In+Cd*). Those rods are then organized in two families, depending on their function : (i) the power shimming rods (PSR) and (ii) the regulation rods (TRR).

The first ones are used to shim the power effects during the power transient, and are split in four groups (four *gray* rods $G1$, eight *gray* rods $G2$, eight *black* rods $N1$ and eight *black* rods $N2$). All the rods of a same group move together, and the groups are inserted successively in this order : $G1$, $G2$, $N1$, $N2$, as it is shown in Fig.3. An overlap is also defined between all the groups, so that they follow an insertion program as illustrated from frames (a) to (d). A convenient definition is used to describe the positions of the four groups using a single value : the totalizer (T). It represents the cumulative number of inserted steps, only incremented by the last moving group. Moreover, the totalizer is linked to the electrical power by a calibration function, established at the beginning of the cycle and updated every 60 equivalent full-power days to take into account the burnup effects. Those rods, however, do not enable to shim the evolution of the Xenon concentration during the transient, as well as the use of the soluble boron.

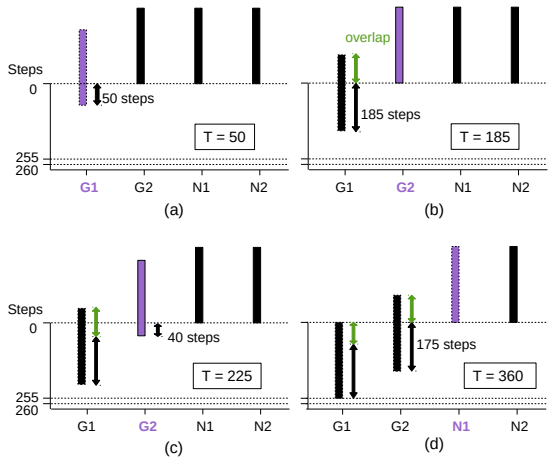

Fig. 3. Insertion sequence of the Power Shimming Rods (PSR). The totalizer value (T) is given on each frame, and the last moving group is in purple.

The second family is made of nine *black* rods gathered in a single group and enables a control of the average coolant temperature of the core (the targeted temperature, called reference temperature, is a linear function of the thermal power). Indeed, the Xenon evolution is managed mainly with the soluble boron, and another family of rods is then needed to cope with the resulting temperature discrepancies. This group moves independently and automatically, following a speed program depending on the difference between the reference temperature (T_{ref}) and the mean temperature (T_m) as shown in Fig.4. One can see a dead band of ±0.8°C in which the rods do not move, avoiding continuous displacement and corresponding to the self-regulation of the core. Finally, as they are very efficient and for safety reasons, they can only move inside a maneuvering band of about 50 centimeters in the upper part of the core. For more details, please refer to [13].

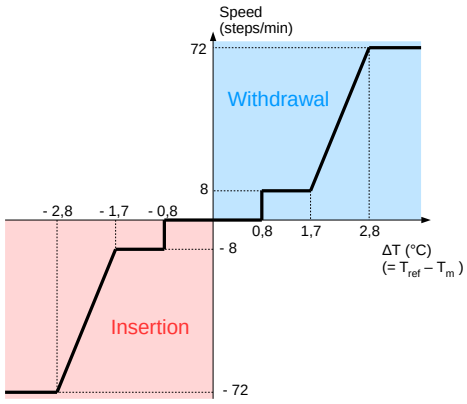

Fig. 4. Speed program of the Temperature Regulation Rods (TRR). The dead band corresponds to the null speed and the maximal and minimal speeds (±72 steps/min) are for an absolute temperature difference larger than 2.8°C.

The variables to be tuned for the optimization are then the four nominal speeds and the three overlaps for the PSR, the maximal and minimal speeds, the dead band width and the maneuvering band height for the TRR. Eleven variables are then considered, and they are coded as integer values corresponding to a discrete number of steps or of temperature (the dead band is discretized by steps of 0.1°C). Tab. I summarizes the variables, their initial values (current management) and ranges.

TABLE I. Integer variables of the design : lower bound (l.), upper bound (u.), and values of the current reference management (r.). The dead band (db) parameter is expressed in tenth of degree, and all the other variables are expressed in steps.

	PSR Overlaps			PSR Velocities				TRR V.		TRR B.	
	o_1	o_2	o_3	v_1	v_2	v_3	v_4	V	v	mb	db
l.	0	0	0	10	10	10	10	42	3	7	8
u.	255	255	255	110	110	110	110	102	13	117	16
r.	70	80	95	60	60	60	60	72	8	27	8

The values in the table take into account some technological and logical constraints. For example, the overlaps cannot be greater than the total height of the rods, the velocity ranges are bounded by the mechanisms, etc. A number of other variables could have been studied, like swaps between groups, or splitting groups, but the study is confined to the variables listed above for two reasons : simplify the problem for a first optimization, and be able to propose a solution without major technological breakthroughs and similar to the current one. Nevertheless, the search domain is huge (at least 3×10^{20} possible configurations).

2. Criteria Definition and Calculation

This seek of simplification is even more understandable when it is known that the black-box evaluation function is very costly. Each unitarian calculation corresponds to a given management configuration running on a complete typical load-following transient, corresponding to about eleven hours. The value of interest is then determined thanks to a model of the whole reactor described in [14], and developed within the APOLLO3® [15] calculation code. The optimization aims at minimizing this value of interest, which represents either a global operating criterion, based on the control diagram, or the rejected volume of effluents. The control diagram is used by the operator to manage the power plant and represents the evolution of the relative thermal power (P_r) as a function of the power axial imbalance ΔI:

$$\Delta I = P_r \times AO$$

where AO is the axial offset defined as $AO = \frac{P_T - P_B}{P_T + P_B}$ and standing for the unbalance between the lower and upper half parts of the core as regards the power. P_T (resp. P_B) is the power in the upper (resp. lower) part of the core.

An example of such a diagram is to be found on Fig.5, which draws the path of the state of the core during a power variation (blue line) and the bounds for this path. On the right side, the forbidden region (red line) is based on many studies and ensures the safety of the core in case of accidental situations. The impossible working region just comes from the definition ($AO \in [-1, 1]$). Finally, the green line starting at the same point as the path corresponds to a constant axial offset, and is called *reference line* in the following.

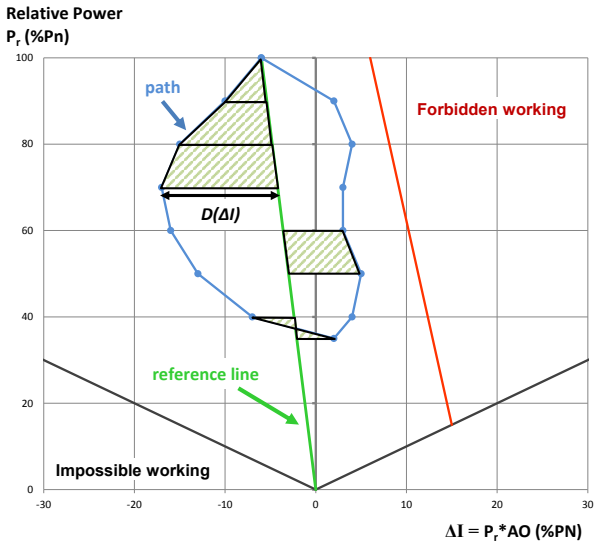

Fig. 5. A control diagram showing the principle of the criterion computation to be minimized. The relative thermal power is expressed in percent of the nominal power ($\%PN$).

The criterion derived from the control diagram is defined by:

$$C_{AO} = \frac{1}{4} \sum_i |P^2_{r,i+1} - P^2_{r,i}| \cdot \Big(D(\Delta I_{i+1}) + D(\Delta I_i) \Big) \qquad (1)$$

where $D(\Delta I_i) = |\Delta I_i - \Delta I_i^{ref}|$. The point $(P_{r,i}, \Delta I_i)$ represents the state of the core at the time step i in the control diagram, and ΔI_i^{ref} the power axial imbalance given by the reference line at the power $P_{r,i}$. The criterion corresponds to the sum of all the areas as illustrated on Fig. 5, weighted by the relative power to take into account the fact that an important axial offset at high power is worse than at low power. Minimizing this criterion enables to reduce the area of the path and avoids being close to the forbidden region while staying close to the reference line.

The second criterion, $V_{\text{effluents}}$, corresponds to the effluents volume produced during the transient. To increase (resp. decrease) the boron concentration in the core, some water of the primary circuit is replaced by highly boron-concentrated (resp. clear) water. Such a boration (resp. dilution) produces a lot of fluid wastes to be processed, called effluents. This volume is determined using the flow rate at which the new fluid is injected (equal to the one at which the current fluid is removed) by the pump :

$$V_{\text{effluents}} = \sum_i Q_i * \Delta t_i$$

where Δt_i and Q_i are the length of the time step and the flow rate (in $m^3.s^{-1}$) of the pump at the time step i. The flow rate is given by :

$$Q_i = -\frac{V}{\Delta t_i} * \log\Big(1 + \frac{[B]_i - [B]_{i-1}}{[B]_{i-1} - [B]^*}\Big) \qquad (2)$$

with V the volume of the primary circuit and $[B]_i$ the boron concentration at the time step i. $[B]^*$ is the concentration of the highly boron-concentrated water (7700 ppm) in case of boration, or of the clear water (0 ppm) in case of dilution.

Both criteria have to be minimized : one wants to reduce as well the axial perturbations on the core and the use of the soluble boron. They are *a priori* contradictory, because an important use of the control rods increases the axial perturbations, but reduces the use of the soluble boron. On the contrary, a limited use of the control rods produces few perturbations, but in that case, the soluble boron is used instead. The optimization process aims at finding a good compromise.

III. ASYNCHRONOUS PARALLEL EA

In this section, we propose a parallel EA dedicated to the NROO problem with computational expensive simulation cost, and to the high performance computing environment composed by a large number of computation units. The parameters of the EA algorithm are also studied.

1. Algorithm Design

Two keys guide the design of the optimization algorithm. First, the time of fitness evaluation computed by the simulator is on average about 40 minutes and with a large variance.

Second, a large number of computing units ($w = 3072$) are available to run the optimization algorithm, but they are available for only few hours (around 15 hours per job [16]). As a consequence, a master-worker (M/W) framework with fitness evaluation on each worker seems to be relevant. Indeed, on average we can expect one fitness evaluation every 0.78 second, meaning that the master node is not to be overflowed by the request of the workers, and with respect to the fitness evaluation time, an idle working time of few seconds will not reduce the performance. In addition, some simulations crash before the end of the calculation, increasing even more the discrepancies in calculation times. All considered, the model of the M/W has been made asynchronous : the workers are updated on the fly without a synchronization barrier, and each worker only computes the fitness value using the multi-physics simulator.

The number of evaluations per worker is small, on average 23 fitness function evaluations is possible on each worker within 15 hours of computation. As a consequence, the EA should converge quickly. We propose then an asynchronous $(1 + \lambda)$-EA where λ is the large number of computation units minus one. Roughly speaking, an iteration of the algorithm produces λ new candidate solutions (which are random variants of the so far best-known solution) by the mutation operator, and updates the best solution for the next iteration. The Algo. 1 and 2 show the details of the algorithm.

Algorithm 1: Asynchronous M/W $(1+\lambda)$-EA on master

for *i in Workers* **do**
  $x^i \leftarrow$ **Initialization** using quasi-random numbers
  Send (non-blocking) Msg(x^i) to worker i
end
$f^\star \leftarrow$ maximal value
while *pending message* ***and*** *time is not over* **do**
  Receive Msg from worker i
  $f^i \leftarrow$ Msg[0]
  if $f^i \leqslant f^*$ **then**
    $x^\star \leftarrow x^i$; $f^\star \leftarrow f^i$
  end
  $x^i \leftarrow$ **Mutate**($x^\star$)
  Send (non-blocking) Msg(x^i) to worker i
end
return $x^\star$

Algorithm 2: Asynchronous M/W $(1 + \lambda)$-EA on workers

Receive (blocking) Msg from master
$x^i \leftarrow$ Msg[0]
$f^i \leftarrow$ **Evaluate** x^i with simulator
Send (blocking) Msg(f^i) to master

First, the algorithm on master node produces $\lambda = w - 1$ quasi-random solutions (integer vectors of dimension $n = 11$) using a Design of Experiments (DoE) based on Sobol of quasi-random numbers. This initialization is used to improve the spreading of the initial solutions in the search space. Every initial solution is then sent asynchronously to a worker, running the Algo. 2 : receive the solution from the master, compute the fitness value by running the multi-physics simulator, and send back the result to the master node. In the meantime, the main loop of the Algo. 1 is executed on the master node : wait for a message from a worker i, and when the fitness value is received, the best so far solution is updated if necessary. Notice that the best solution is replaced by the new solution evaluated by the worker even when the fitness values are equals. In that way, the algorithm is able to drift on plateaus of the search space which are solutions with the same criterion value. A new candidate solution is then computed by the mutation operator of the best-known solution and sent in non-blocking mode to the same worker i. The master is then able to manage the requests of the other worker nodes by the asynchronous communication mode. The stopping criterium of the algorithm is the time limit.

The mutation operator is based on the classical mutation operator for vectors of numbers. The mutation rate p defines the parameter of the Bernouilli distribution to modify each number of the vector. Therefore, the number of modified variables follows a binomial distribution of parameters n and p, and the expectation of the number of modified variables is np. When an integer variable is modified according to the mutation rate, a random integer number is drawn using a uniform distribution centered on the current value. Let x_j be the current value of the variable j, and δ_j the gap defined by $\lfloor r.(ub_j - lb_j) \rfloor$ where lb_j and ub_j are respectively the lower bound and the upper bound of the variable j defined in the Tab. I, and $r \in [0, 1]$ is a mutation parameter. The new integer value of variable j after mutation is selected uniformly in the interval $[x_j - \delta_j, x_j + \delta_j] \cap [lb_j, ub_j] \setminus \{x_j\}$. The parameter r tunes the range width for the new value of variable after the mutation, and is expressed relatively to the total range width of the parameters.

In addition, to avoid multiple costly evaluations of the same candidate solution, a hash-map is used on the master node to save all evaluated solutions. The mutation is applied on the solution until a new candidate solution which is not in the hash-map is produced by the mutation random process.

2. Parameters Tuning

First, the performance of the algorithm with a *baseline* parameters setting is studied with 3072 computing units during 24 hours (approx. 73, 728 hours of CPU time). Following the value of the mutation rate parameter of $1/n$ commonly used in EA, the mutation rate has been set roughly to the inverse of the number of variables ($p_0 = 0.1$), so that the mutation operator modify on average one variable. The width of the random variation range has been arbitrarily set to about $r_0 = 0.05$ (5% of the total variation range of the variable).

The use of an asynchronous algorithm to avoid idle time is justified by the discrepancies of the computation costs from a candidate solution to another one : the mean computation time is 2426 seconds, and the faster computation is done in 1629 seconds whereas the longer is performed in 6169 seconds.

Fig.6 shows the dynamic of the run. The C_{AO} value is

drawn as a function of the number of evaluations received by the master node. A point is plotted when the best solution so far is updated (included for equal fitness values) and the fitness values are normalized by the fitness value of the current management (see Tab. I). The solutions for which the number of evaluations is lower than 3072 are from the initial quasi-random population. Even if the *baseline* settings enable to reduce the fitness of about 40% compared to the current management, it can be seen that the number of strictly improving solutions is low (about 10 improving steps). The dynamic is a punctuated equilibrium dynamic with a lot of plateaus (made of solutions of the same quality), and therefore few improving solutions. For instance, the process is stuck on a plateau at the end of the run and almost $50,000$ fitness evaluations are necessary to find another plateau with strictly better solutions. This first experiment shows the relevance of the algorithm to find better solutions than the current management, but it also suggests that the settings of the mutation parameters could be improved.

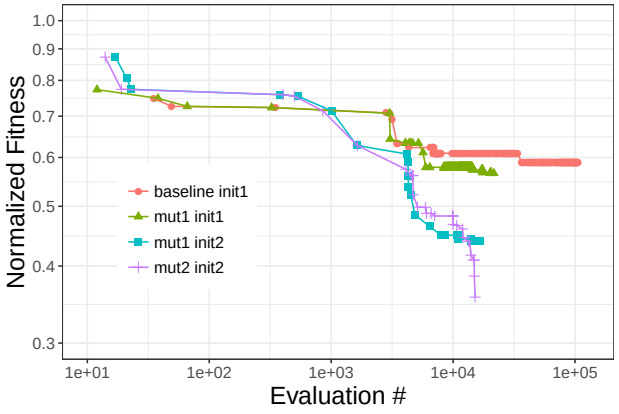

Fig. 6. Evolution of the normalized fitness as a function of the number of evaluations for some mutation parameters settings, and starting populations. Notice the log scale

Four values of mutation rates p and mutation ranges r are then investigated : $p \in \{0.1, 0.2, 0.3, 0.4\}$ and $r \in \{0.05, 0.1, 0.2, 0.5\}$. All the combinations are considered, given 16 possible mutation settings of the mutation operator. Moreover, to reduce the intrinsic random effect of the algorithm, each couple of mutation parameters values (p,r) have been launched five times with different initial populations generated by the Sobol sequence of quasi-random numbers. However, the five initial populations are the same for each couple of parameters settings. The algorithm is launched this time on 3072 computing units during five hours (approx. $15,360$ hours of CPU time per run), giving a total computation cost of more than $1,2 \times 10^6$ hours of computation, and it was not possible to execute more than five runs per mutation settings.

Two sets of mutation parameters are shown on Fig.6 (*mut1* and *mut2*). The first set corresponds to $(2p_0, 2r_0)$, and is shown starting either from the same population as the *baseline* settings (*init1*), or from another pseudo-random population (*init2*). The second set is the best set found with this parametric study and corresponds to $(3p_0, 10r_0)$.

The (*mut1*, *init1*) configuration is better than (*baseline*, *init1*), and enables to find another local minimum. In the same way (*mut2*, *init2*) is better than (*mut1*, *init2*). By increasing the mutation rate p and the random range r, one increases the differences between a solution and his mutant, improving the exploration phase. On the other hand, lower mutation rate and random range improve the exploiting around a good solution. Given the computing time, the number of cores, and the algorithm structure, it appears that the better the exploration, the better the solution. The initial population has also a huge influence on the solution, as it can be seen between (*mut1*, *init1*) and (*mut1*, *init2*).

One can see the importance of optimizing the parameters of the algorithm : a gain of about 65% is reached against 40% with the *baseline* settings.

IV. EXPERIMENTAL ANALYSIS

1. Mono-objective Optimizations

This section deeply analyzes the optimizations with respect to both criteria. To do so, the optimization process is launched again in order to optimize this time the effluents volume. The parameters of the algorithm are the one corresponding to the so far best configuration, which is (*mut2*, *init2*). The dynamic of the optimization is similar to the one for the axial offset criterion, and is not presented here. This optimization results and the ones coming from the best run as regards the axial offset criterion are then gathered (all the solutions are kept, and not only the improving ones as in Fig.6), and the Pareto set is built. The Pareto set is made of all the *non-dominated* (or *Pareto-optimal*) solutions. Let $\mathcal{X}$ be the search space, and $f : \mathcal{X} \to \mathbb{R}^n$ the fitness function which associates to each candidate solution the scalar values to be minimized (here $n = 2$). A solution x in search space is said *dominated* by a solution x' if :

$$\forall i \in \{1, \ldots, n\} \mid z'_i \leq z_i \text{ and } \exists j \in \{1, \ldots, n\} \mid z'_j < z_j$$

where $z' = f(x')$ and $z = f(x)$. A solution x is then *non-dominated* if there does not exist any solution x' that dominates it. The set of Pareto-optimal solutions is the Pareto set, and its mapping in objective space is the Pareto front, which is shown in Fig.**??** for the gathered optimization results.

It is satisfactory to see that the two mono-objective optimizations give a well-distributed front, and that the two optimizations contribute almost the same way to the front (same number of points from the optimization as regards C_{AO} than $V_{\text{effluents}}$). The two criteria are contradictory as expected, since an optimization with respect to one degrades the other. Moreover, the current management is well improved for both criteria, and is dominated by about 15 points. It is interesting, however, to note that the Pareto front is centered around the current management, meaning that this management can be seen as an already improved solution as regards those two criteria.

Three candidate solutions are pointed out on this Pareto front : the one giving the best axial offset criterion (*best AO*), the one giving the best effluents volume (*best Veff*), and one in the middle of the Pareto front (at (0.75,0.8)) called *best*

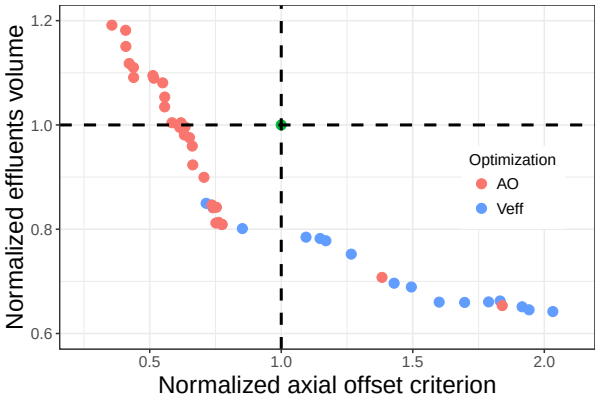

Fig. 7. Pareto front obtained with the mono-objective optimizations as regards both criteria. The points coming from the two optimizations are distinguished. The values are normalized with the ones of the current management, which is at the center of the dotted cross.

Compromise, giving one of the best compromise between the two criteria, and dominating the current management. Fig.8 presents the corresponding control diagrams, and the evolution of the soluble boron concentration all along the load-following transient. It was said previously that the volume of effluents characterizes the use of the soluble boron, and consequently, the less the amplitude of the soluble boron concentration, the less the rejected volume of effluents.

First of all, Fig.8 (top) shows that the area of the *best AO* path is well reduced (65% reduction) compared to the current management, and the axial offset stays very close to the reference line. In comparison, even if the area of the path of *best Veff* is small, the curve stays far from the reference line, explaining why C_{AO} is important for this solution. As expected, *best Compromise* is between the two : reducing the use of the soluble boron but still ensuring a good behavior of the control diagram. The "S" shape of all the control diagrams excepted the *best AO* is due to the differential worth discrepancies of the PSR. One can avoid this effect by modifying their overlaps so that the reactivity insertion from one group to another is done in a smoother way, but also by reducing the velocities in such a way that the rods do not reach their expected position (given by the calibration function), reducing their axial effects on the core. Their final position is reached once finished the power variation. However, this strategy implies an important use of the soluble boron, which is used to shim the power effects (instead of the PSR), as it can be seen on Fig.8 (bottom) from point *A* to *B* where the boron concentration increases. On the contrary, an important use of the PSR to shim the power effects like for *best Veff*, leads to a reduced use of the soluble boron (variation of 120 ppm in the case of *best AO* compared to 60 ppm for *best Veff*).

Tab. II summarizes the parameters of the three previous candidate solutions, and remind the one of the current management. The overlaps of the *best AO* management are slightly higher than the current management ones, implying *a priori* higher perturbation on the core (a maximal overlap between

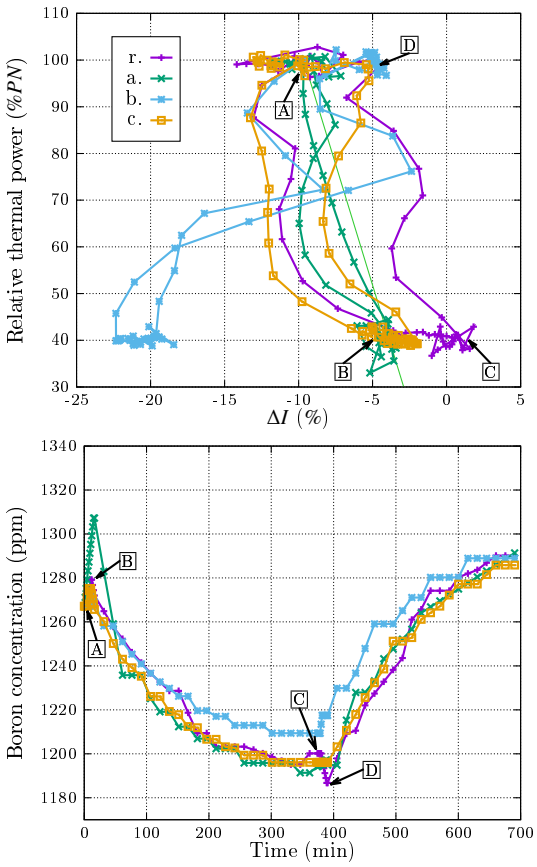

Fig. 8. Control diagram and evolution of the soluble boron concentration for the three candidate solutions of the Pareto front, and for the current management. Current reference management (r.), *best AO* (a.), *best Veff* (b.) and *best Compromise* (c.). The A, B, C and D points corresponding to the power transient are indicated on the control diagram of the current management.

two groups means that they are inserted together, contrary to a null overlap meaning that the first one is completely inserted before the second one starts moving). This is avoided by setting the $G1$ velocity to its minimal value, so that the rods cannot reach their expected position. Consequently, during the power decrease for instance, they are not enough inserted, meaning fewer effects on the core. Plus, the maneuvering band of the TRR is thin so they cannot be used neither. The boron is then used instead, and its almost uniform effect on the core explains why *best AO* ensures a path very close to the reference line, meaning that the axial offset is kept almost constant.

The *best Veff* configuration, however, maximizes the use of the PSR : $G1$ is inserted alone and when it reaches the bottom of the core, the power is around $75\%PN$. From that point, $G2$ and $N1$ are inserted together, and $N2$ starts moving shortly after them. This produces a huge decrease of the axial offset, as it can be seen on Fig.8 (top). Moreover, the maneuvering band of the TRR is wide, so that the use of the

soluble boron in this case is reduced to the minimum. Finally, the *best Compromise* configuration appears to be very close to the *best AO*, and the main difference is for the PSR velocities : with higher velocities, the power shimming is better, enabling to reduce the use of soluble boron.

TABLE II. Summary of the parameters of the previous candidate solutions : current reference management (r.), *best AO* (a.), *best Veff* (b.) and *best Compromise* (c.).

	PSR Overlaps			PSR Velocities				TRR V.			
	o_1	o_2	o_3	v_1	v_2	v_3	v_4	V	v	mb	db
r.	70	80	95	60	60	60	60	72	8	27	8
a.	113	84	215	10	67	26	91	68	11	8	13
b.	1	253	202	42	109	47	47	47	7	93	12
c.	113	83	74	85	78	97	60	76	11	12	9

In order to generalize the comments made on the parameters of the three candidate solutions of the Pareto front, other candidate solutions are considered. For both optimization process (as regards C_{AO} and $V_{\text{effluents}}$), all the solutions under a chosen normalized value are taken into account. This limit is set to 0.6 in case of C_{AO}, and 0.75 in case of $V_{\text{effluents}}$. The two values are different because the variation ranges on the two criteria are different, and the choice is made so that only the best solutions are kept, without removing too many solutions. Moreover, the number of kept solutions in both cases is almost the same (about 1350 solutions). Fig.9 shows the parameter values distribution for the solutions found during the C_{AO} optimization (left) and the $V_{\text{effluents}}$ optimization (right).

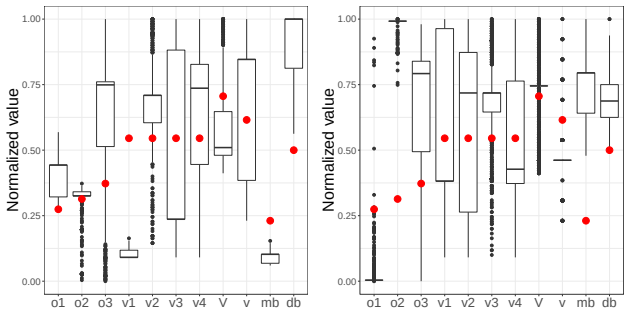

Fig. 9. Summary of the parameter values for the best solutions found with the C_{AO} (left) and $V_{\text{effluents}}$ (right) optimization. The bottom (resp. top) of the boxes corresponds to the first (resp. third) quartiles, and the lower (resp. upper) whiskers extend from the boxes to the lowest (resp. highest) value within 1.5 times the distance between the first and third quartile. Values beyond or above are plotted as points. The median values are represented by the horizontal segments inside the boxes. The red points correspond to the current management.

In both cases, the parameters $o3$, and $v4$ seem to have almost no influence on the values of interest, as the corresponding standard deviations are high. This can be explained by the fact that $N2$ is only used in few management configurations. Particular attention must be paid to the values of $o1$, $o2$, $v1$ and *mb*, which are the values that present the main discrepancies between the two optimizations. On Fig.9 (left), the first quartile of the overlaps is always higher than the current management. For $o1$, the current management corresponds even to the lowest value. Moreover, the values of $v1$ and *mb* are close to the minimum. Consequently, the previous discussion on the strategy of the *best AO* management can be generalized to the good solutions found as regards C_{AO} : by decreasing the velocity of the rods and the maneuvering band, one imposes the use of the soluble boron as the main control mechanism, and thus enable to improve the axial offset criterion. Keeping high overlaps opens, nevertheless, the possibility to decrease the use of the soluble boron by increasing the velocities. In the same way, the discussion on the strategy of the *best Veff* management is verified here, as it can be seen that $o1$ is minimal and $o2$ is maximal excepted for few solutions. On the one hand, the overlaps must be high in order to have a good shimming effect, as it is the case for *best Veff*, and leading to a reduced used of the soluble boron. The TRR enable to control the resulting average temperature and axial offset, and a high maneuveuring band is thus needed. But on the other hand, a too strong impact of the PSR on the core may also require the use of the soluble boron, which would increase the effluents volume, and that is probably why the first overlap is kept low.

2. Influence of the Burnup

The soluble boron is also known to be used to counterbalance the decrease of reactivity all along the cycle, and its concentration never stops decreasing during the cycle. Usually, the maximum burnup for the load-following is given by a minimum amount of soluble boron left in the core. After a given burnup (about 80% of the cycle length), the reactor is not able anymore to load-follow, because the remaining soluble boron is not enough to counterbalance the Xenon effect. Moreover, the principle of boration and dilution of the soluble boron (Eq. (2)) implies that at low concentration, the boration is fast and the dilution is low. Consequently, at high burnup, a fast dilution is not possible, and that could also limit the possibilities of a core to load-follow. One can deduce that the burnup has an important effect on the performances of the solutions, especially if the use of the boron differs from a solution to another. As it is difficult to change online the management during the cycle, a candidate solution must be good all along the cycle to be chosen. Here, the robustness of the solutions with respect to the burnup is studied, by replaying the load-following transient for the solutions in the Pareto set, but with different initial states of burnup. The control diagrams of the *best AO*, *best Veff* and current management configurations are shown on Fig.10, and correspond to a load-following starting at 80% of the cycle length. The *best Veff* configuration is better than either the current management and *best AO* for both criteria. Its control diagram shape is the same as in Fig.8 (top) : by minimizing the use of the soluble boron and maximizing the use of the control rods, one enables robustness as regards the burnup. When starting with a core at high burnup, the managements that need more soluble boron are consequently penalized. This is what Fig.10 shows. For

the current management and *best AO*, the needed boration and dilution speeds cannot be reached, making it difficult to fully counterbalance the power effects during the power decrease, and the xenon effect during the lower plateau. This is the cause of the drift observed during the lower plateau, resulting in a high C_{AO} value.

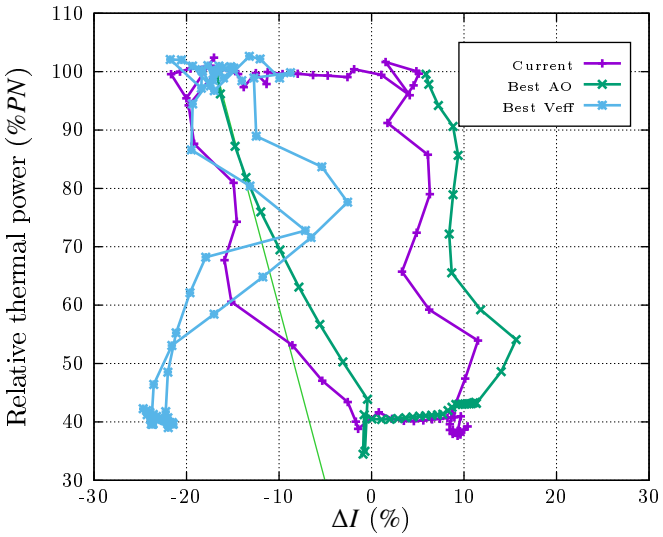

Fig. 10. Control diagrams for the current management, *best AO* and *best Veff* at 80% of the cycle length.

Knowing the importance of the burnup on the values of interest for those three management configurations, the effect of the burnup on the whole Pareto front is now shown in Fig.11. From top to bottom, the initial burnup increases from 20% to 50% and then 80% of the cycle length (CL), and its effects on the front can be seen thanks to the color scale. The circle points stand for the initial Pareto front, and the triangle for the same management configuration, starting from the corresponding increased burnup. The references are at the center of the dotted cross.

As expected, the effect of the burnup on the Pareto front is important. Surprisingly, the more the burnup, the fewer the effects on the whole front. Even if the huge majority of the solutions is dominated by the initial Pareto front, some dominate it, meaning, as we discussed before that the effects are not uniform from a solution to another. More precisely, the color scale shows that the solutions optimized as regards the effluents volume tend to be improved as the burnup increases, whereas the solutions optimized as regards the axial offset criterion tend to be degraded. Indeed, the $V_{\text{effluents}}$-optimized solutions start from the bottom right corner and go to the bottom left corner, meaning that they dominate the current management, whereas the C_{AO}-optimized solutions start from the top left corner and go to the top right corner, meaning that they are dominated by the current management, and thus by the $V_{\text{effluents}}$-optimized solutions. The solutions in the middle of the front stay close, most of the time, from the current management. The behavior of the Pareto front as a function of the burnup is still not well understood, but the final state (at

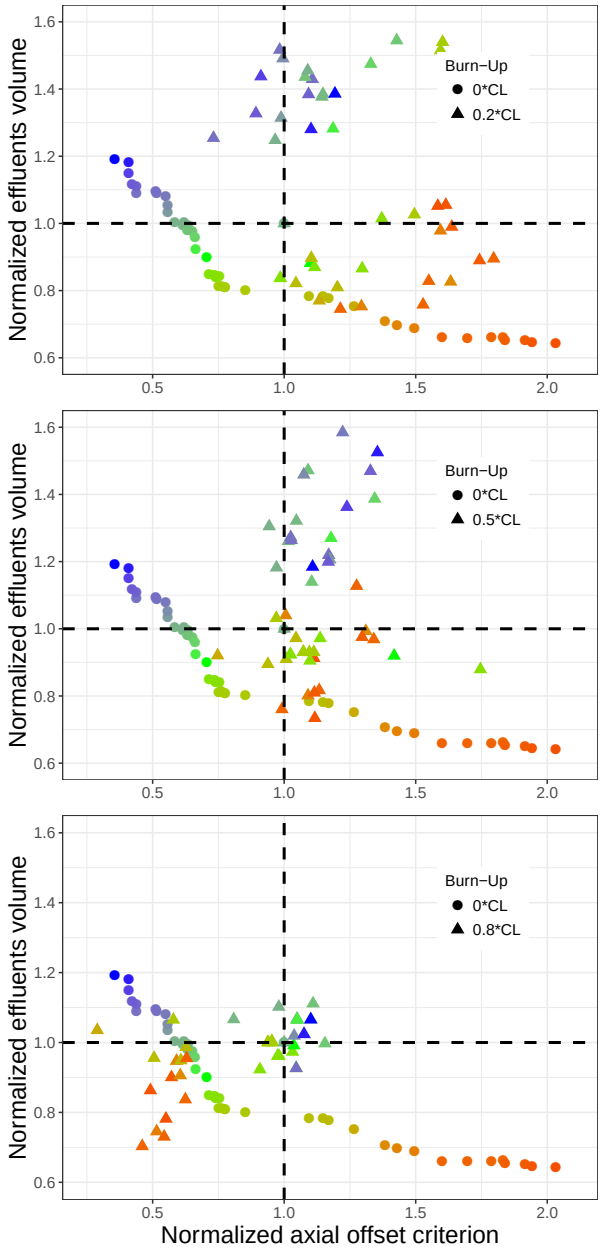

Fig. 11. Effects of an increasing burnup on the Pareto front. 0.2CL (top), 0.5CL (middle) and 0.8CL (bottom). The values corresponding to managements starting from an increased burnup are normalized with respect to the values of the current management, starting from the same increased burnup.

80% of the cycle length) corresponds to the discussion above. The absolute axial offset criterion of the $V_{\text{effluents}}$-optimized solutions do not change much, whereas the value of the current management increases, making the normalized axial offset criterion decrease, and the normalized effluents volume of those solutions stays lower the one of the current management. Concerning the C_{AO}-optimized solutions, the normalized effluents volume stays almost constant also (or slightly increases), but

most of all, the axial offset criterion is increased, and gets closer to the reference. Fig.10 shows indeed that the *best AO* and current managements are very similar to each other. One can conclude that the $V_{\text{effluents}}$-optimized solutions are more robust than the C_{AO}-optimized solutions as regards the burnup. It is not possible, however, to simply choose those solutions, because Fig.8 shows that the maximal corresponding axial offset may be important, which is not acceptable with respect to the safety, particularly linear power and xenon oscillations. Consequently, the gathering of the two mono-objective optimizations is not enough (because not robust enough as it has been shown), and a bi-objective optimization is needed to find a compromise between $V_{\text{effluents}}$-optimized solutions and acceptable axial offset variations.

V. CONCLUSIONS

A study concerning the optimization of the management of a Pressurized Water Reactor during a load-following transient have been presented, and the first results demonstrate the possibility of an improvement of the current management as regards two criteria which are the effluents volume and a criterion based on the axial offset calculation. It has been possible to improve the later by 65% and the former by 40%. However, some work is still to be done in order to optimize them jointly, and find good solutions as regards the two criteria. Those solutions will have, moreover, to be efficient as far as possible in the cycle length.

This is the next step of the work : develop a multi-objective algorithm, based on the mono-objective one, enabling to find those solutions. The optimization will be done considering the beginning of the cycle in a first time, as it was the case here, and increased burnups in a second time. By comparing the results of those two bi-objective optimization, one will be able to point out the common solutions, thus efficient for the several burnups.

VI. ACKNOWLEDGMENTS

APOLLO3® is a registered trademark of CEA.

The authors would like to thank IDEX and PS2E for their financial support. The authors gratefully acknowledge AREVA and EDF for their long-term partnership and their support. This work was performed using HPC resources from GENCI-TGCC (Grant 2016-t2016107616).

The authors would especially like to thank Hubert Grard from INSTN for his help in the setting of the simulator as well as for his precious advises concerning the analysis of the results.

REFERENCES

1. O. DUMONT, "Ademe Energie 2030 : Production d'énergies renouvelables," Tech. rep., Ademe (2012).
2. G. ARNAUD, J.-M. DO, J.-J. LAUTARD, A.-M. BAUDRON, and S. DOUCE, "Selection Combinatory Algorithm for Loading Pattern Design of Light Water Reactor with Two Levels of Heterogeneity," *Proceedings of ICAPP 2011 Nice, France (Paper 11091)* (2011).
3. A. A. DE MOURA MENESES, L. M. GAMBARDELLA, and R. SCHIRRU, "A new approach for heuristics-guided search in the In-Core Fuel Management Optimization," *Progress in Nuclear Energy, Vol. 52* (2010).
4. C. M. PEREIRA and C. M. LAPA, "Coarse-grained parallel genetic algorithm applied to a nuclear reactor core design optimization problem," *Annals of Nuclear Energy, Vol. 30* (2003).
5. W. F. SACCO, C. R. DE OLIVEIRA, and C. M. PEREIRA, "Two stochastic optimization algorithms applied to nuclear reactor core design," *Progress in Nuclear Energy, Vol. 48* (2006).
6. W. F. SACCO, C. M. LAPA, C. M. PEREIRA, and H. A. FILHO, "A Metropolis Algorithm applied to a Nuclear Power Plant Auxiliary Feedwater System surveillance tests policy optimization," *Progress in Nuclear Energy, Vol. 50* (2008).
7. M. G. NA, I. J. HWANG, and L. Y. JOON, "Design of a Fuzzy Model Predictive Power Controller for Pressurized Water Reactors," *IEEE Transactions on Nuclear Science, Vol. 53 (3)* (JUNE 2006).
8. J. H. KIM, S. H. PARK, and M. G. NA, "Design of a model predictive load-following controller by discrete optimization of control rod speed for PWRs," *Annals of Nuclear Energy, Vol. 71* (2014).
9. E. ALBA and M. TOMASSINI, "Parallelism and evolutionary algorithms," *IEEE Transactions on Evolutionary Computation*, **6**, *5*, 443–462 (2002).
10. M. DUBREUIL, C. GAGNE, and M. PARIZEAU, "Analysis of a Master-Slave Architecture for Distributed Evolutionary Computations," *IEEE T. on Systems, Man, and Cybernetics: Part B*, **36**, 229–235 (2006).
11. S. WESSING, G. RUDOLPH, and D. A. MENGES, "Comparing Asynchronous and Synchronous Parallelization of the SMS-EMOA," *J. Handl et. al. (Eds.), Springer International Publishing, PPSN XIV* (2016).
12. A. LOKHOV, "Technical and economic aspect of load following with nuclear power plants," *Nuclear Energy Agency, OECD* (June 2011).
13. H. GRARD, *Physique, fonctionnement et sûreté des REP*, EDP Sciences (2014).
14. M. MUNIGLIA, J.-M. DO, J.-C. LE PALLEC, H. GRARD, S. VEREL, and S. DAVID, "A multi-physics PWR model for the load following," *ICAPP* (2016, San Francisco, California).
15. D. SCHNEIDER, F. DOLCI, F. GABRIEL, and J.-M. PALAU, "Apollo3® : CEA/DEN deterministic multi-purpose code for reactor physics analysis," *PHYSOR* (Sun Valley, IDAHO, May 1-5, 2016).
16. `http://www.genci.fr/en`.